

Low-field-enhanced unusual hysteresis produced by metamagnetism of the MnP clusters in the insulating CdGeP₂ matrix under pressure

T. R. Arslanov,^{1,*} R. K. Arslanov,¹ L. Kilanski,² T. Chatterji,³ I. V. Fedorchenko,^{4,5} R. M. Emirov,⁶ and A. I. Ril⁵

¹*Amirkhanov Institute of Physics, Dagestan Scientific Center, Russian Academy of Sciences (RAS), 367003 Makhachkala, Russia*

²*Institute of Physics, Polish Academy of Sciences, Aleja Lotnikow 32/46, PL-02668 Warsaw, Poland*

³*Institute Laue-Langevin, Boîte Postale 156, 38042 Grenoble Cedex 9, France*

⁴*Kurnakov Institute of General and Inorganic Chemistry, RAS, 119991 Moscow, Russia*

⁵*National University of Science and Technology MISiS, 119049, Moscow, Russia*

⁶*Dagestan State University, Faculty of Physics, 367025 Makhachkala, Russia*

(Received 11 April 2016; revised manuscript received 28 October 2016; published 22 November 2016)

Hydrostatic pressure studies of the isothermal magnetization and volume changes up to 7 GPa of magnetic composite containing MnP clusters in an insulating CdGeP₂ matrix are presented. Instead of alleged superparamagnetic behavior, a pressure-induced magnetization process was found at zero magnetic field, showing gradual enhancement in a low-field regime up to $H \geq 5$ kOe. The simultaneous application of pressure and magnetic field reconfigures the MnP clusters with antiferromagnetic alignment, followed by onset of a field-induced metamagnetic transition. An unusual hysteresis in magnetization after pressure cycling is observed, which is also enhanced by application of the magnetic field, and indicates reversible metamagnetism of MnP clusters. We relate these effects to the major contribution of structural changes in the composite, where limited volume reduction by 1.8% is observed at $P \sim 5.2$ GPa.

DOI: [10.1103/PhysRevB.94.184427](https://doi.org/10.1103/PhysRevB.94.184427)

In recent years, successful integration of ferromagnetism with semiconductors has focused on ferromagnetic-semiconductor hybrid structures consisting of metallic ferromagnets embedded into a semiconducting host. These materials appear to have significant advantage due to their high Curie temperature compared to conventional diluted ferromagnetic systems [1,2]. Furthermore, the huge magnetoresistance (MR) [3–5], the tunneling MR [6,7], and large magneto-optical effects [8,9] in such hybrid composites make them excellent candidates for the development of new concept magneto-electronic devices. In particular, the useful properties for device applications such as spin-dependent transport [10,11] or spin-polarized tunneling based on the modified magnetic tunnel junction [12,13] could be greatly improved using local magnetic clusters.

It is conceivable that the transport, structural, and magnetic characteristics of hybrid materials may be tuned through the cluster size, cluster shape, and the mean distance between clusters in the surrounding matrix. In this context, studies of nanoscaled MnAs clusters embedded in a GaAs matrix [14–20] provide a test ground for tailoring materials with specific cluster configurations [21]. For example, ordered arrangements of cluster chains consisting of elongated MnAs nanoclusters grown by selective-area metal-organic vapor-phase epitaxy exhibit a large positive MR at low temperatures [19]. On the other hand, a formation of Mn nanocolumns with a spacing of 10 nm in Ge:Mn exemplifies the case of natural cluster self-organization, which leads to a giant MR effect up to 200% at room temperature [5]. Another point of view on this issue is that the self-organization can be achieved artificially. An effective tool in this respect is the hydrostatic pressure, which enables the clusters response to be customized due to prolonged changes in the host matrix. Current

research shows that submicron MnAs and MnP clusters in a chalcopyrite CdGeX₂ ($X = \text{As}, \text{P}$) host exhibit a very high sensitivity to pressure application, allowing their magnetic and transport properties to be controlled [22,23]. At the same time, pressure-induced changes occurring in the host matrix, e.g., structural [24,25] or insulator-to-metal transitions [26], may offer interesting opportunities as well as physical insight into the self-organization/reorganization processes of clusters in the hybrids. Very recently, we found that the structural transition in Mn-doped ZnGeAs₂ produced inversion in the magnetization hysteresis direction (due to MnAs clusters) that was accompanied by remarkable changes in the large MR [27]. Such an unusual manifestation of hysteresis has previously been classified as an intrinsic feature of perovskite structures [28]. In the presence of magnetic inhomogeneities, the reasons driving this unusual hysteresis related to the chalcopyrite host are assigned either to competing interactions between two types of MnAs clusters or their bulk properties. Therefore, it is important to elucidate if this unusual hysteresis is a general trend for chalcopyrite-based hybrids and the mechanism that results in its occurrence.

Here, we report combined high-pressure and low-magnetic-field studies of the isothermal magnetization of a CdGeP₂ matrix containing one type of MnP cluster at Mn doping as high as 12%. We reveal that the maximum zero-field magnetization at $P = 3.5$ GPa is associated with the pressure-induced antiferromagnetic state of the MnP clusters, followed by field-induced metamagnetism. In agreement with our observation [27], an unusual magnetization hysteresis during the pressure cycling was also observed, showing gradual enhancement in the low-field regime. We show that the volume collapse by $\sim 1.8\%$ at $P \approx 5.5$ GPa in the composite is the primary reason for this hysteresis, which leads to different relaxation rates of both clusters and host matrix.

A polycrystalline sample of CdGeP₂-MnP was prepared by direct fusion method. Details of the synthesis were described

*Corresponding author: arslanovt@gmail.com

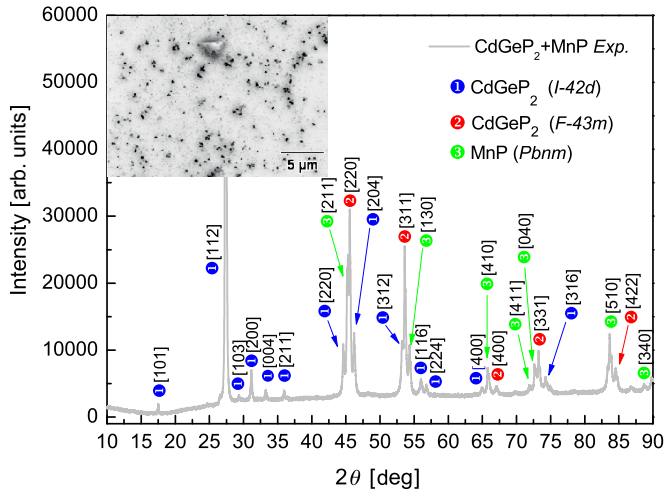


FIG. 1. Room-temperature XRD diffraction patterns of the CdGeP₂-MnP composite. The inset shows SEM image.

elsewhere [29]. In the present paper, we reached a high Mn impurity content with 12% concentration, at which the host CdGeP₂ structure is phase-separated by MnP clusters. Since the semiconducting properties of CdGeP₂ at such levels of MnP clusters begin deteriorating and become close to insulating, the room temperature resistance of the composite was about ~ 1 G Ω . Figure 1 shows the powder x-ray diffraction (XRD) patterns with Miller indices corresponding to three phases present in the crystal. In addition to the well-indexed tetragonal chalcopyrite phase of CdGeP₂ (*I*-42*d*), with lattice parameters $a = 5.738$ Å and $c = 10.766$ Å, we observed a small amount of inclusion of the cubic CdGeP₂ (*F*-43*m*) structure, with lattice parameter $a = 5.592$ Å. Note that the

cubic CdGeP₂ structure is derived from a high-temperature modification of the tetragonal structure [30]. The third phase with the orthorhombic MnP (*Pbnm*) structure and lattice parameters $a = 5.905$ Å, $b = 5.249$ Å, and $c = 3.167$ Å can be successfully distinguished from XRD data and is also presented in Fig. 1. The presence of MnP clusters in the sample was also confirmed by means of scanning electron microscopy (SEM). According to the SEM image, orthorhombic MnP clusters with an average size less than 1 μ m were randomly distributed in the host matrix (inset to Fig. 1).

AC-magnetization measurements under applied hydrostatic pressures up to 7 GPa were carried out in a Toroid-type high-pressure cell [27,31]. For generation of magnetic field up to 5 kOe, we employed an external helical coil. Small CdGeP₂-MnP crystals (with a length of 3 mm and diameter of 1 mm) were inserted in inductively coupled small coils and loaded together with a manganin wire for pressure monitoring into a Teflon capsule of 80 mm³ volume. Volumetric measurements were performed on the sample, which was $3 \times 1 \times 1$ mm³ in size, by using an accurate strain-gauge technique [32]. In all experiments, a mixture of ethanol:methanol 4:1 was used as the pressure-transmitting medium, which remains liquid up to 10 GPa at room temperature and ensures highly hydrostatic pressure production.

Figure 2(a) displays the pressure-dependent normalized magnetization (M/M_0 , where M_0 is the value of magnetization at 0 GPa) of CdGeP₂-MnP measured at ambient temperature under applied low fields up to $H = 5$ kOe. It is noteworthy that at zero magnetic field, there is a maximum of pressure-induced magnetization at $P^{\max} = 3.5$ GPa. The P^{\max} is markedly shifted to lower pressures with the applied field (see Table I). Although the observed characteristics are reminiscent of a superparamagnetic response of the MnP

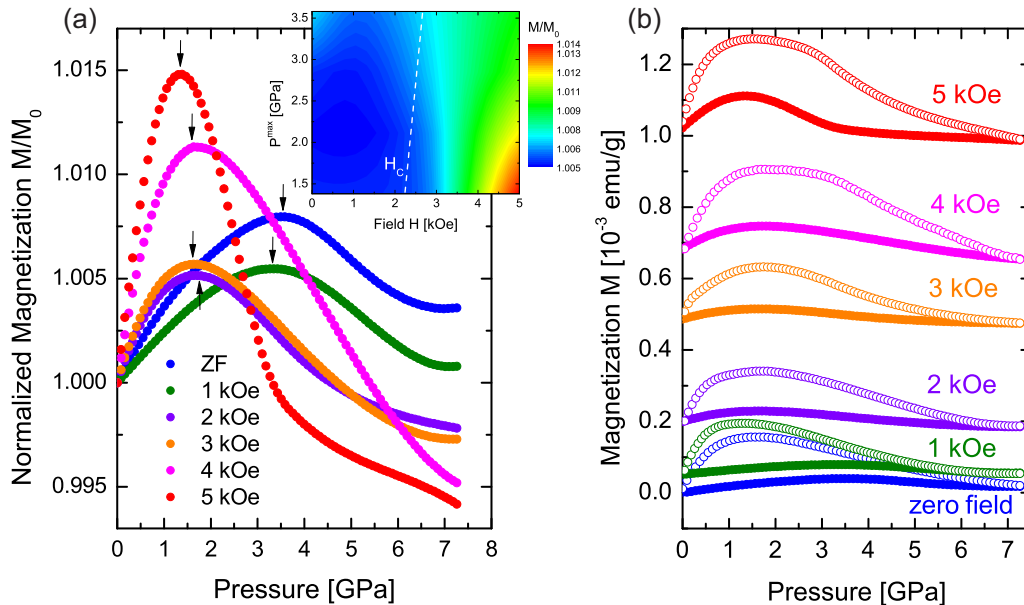


FIG. 2. Pressure dependencies of normalized M/M_0 (a) and absolute (b) magnetization (after subtraction of zero field contribution) measured at applied magnetic field of $H = 0$ –5 kOe and room temperature. A variation in M/M_0 as a function of the maximum positions of P^{\max} and H is represented in the inset to (a). Dashed line corresponds to the critical field H_c within the pressure window of P^{\max} as further defined from Fig. 3. Clear hysteresis behavior of absolute magnetization during pressure cycling (compression = closed circles and decompression = open circles) is shown in (b).

TABLE I. The value for the maximum pressure (P^{\max}) deduced from the pressure-dependent normalized magnetization (M/M_0) at different applied fields (H), including their pressure coefficients.

H (kOe)	P^{\max} (GPa)	M/M_0	dH/dP (kOe/GPa)	$(1/M_0)(dM/dP)$ (GPa $^{-1}$)
0	3.58	1.007		
1	3.34	1.0054		
2	1.71	1.0051	-0.9	6.9×10^{-4}
3	1.63	1.0056		
4	1.6	1.011		
5	1.38	1.014	-8.52	-0.027

clusters in the insulating CdGeP₂ matrix, the appearance of magnetization in zero field excludes this possibility. Together with the contour map shown in the inset to Fig. 2(a), the position of $P^{\max} = 1.38$ GPa at a magnetic field of $H = 5$ kOe indicates an increase in the value of M/M_0 . As presented in Table I, in the range of fields $H = 0-2$ kOe, an intermediate reduction of M/M_0 predominates. Estimation of the pressure coefficient of dH/dP points to a change in the rate from -0.9 kOe/GPa to -8.52 kOe/GPa in the field ranges of $0-2$ kOe and $2-5$ kOe, respectively. For the pressure coefficient $(1/M_0)(dM/dP)$, we found a change in the slope with opposite sign from $+6.9 \times 10^{-4}$ GPa $^{-1}$ to -0.027 GPa $^{-1}$ for the same ranges of fields. Consequently, such behavior is caused by the pressure-field-induced magnetic transition associated with MnP clusters, rather than the conventional magnetization process of clusters that is characteristic of field-induced superparamagnetism.

Figure 2(b) shows the hysteresis behavior for the absolute magnetization after pressure cycling at different magnetic fields. The main feature of this type of hysteresis is that the direction of magnetization at decompression occurs on top against the compression stroke, as previously observed [27]. One can see that the application of the low field leads to enhancement of unusual hysteresis. In addition, this hysteresis characteristic confirms the presence of the first-order magnetic phase transition. However, the origin of the magnetic transition itself is not clear at this stage. To this end, we studied the magnetization $M(H)$ curves, which can provide a definite conclusion about the spin ordering of the MnP clusters under pressure.

The behavior of $M(H)$ isotherms collected for different pressures at compression and decompression is shown in Fig. 3 (upper panels). For the best representation, the contribution of the zero field has been subtracted from each $M(H)$ dependency. As can be seen, a possible ferromagnetic or superparamagnetic signature for MnP clusters in the measured fields of $H \leq 5$ kOe has not been identified. Instead, all isotherms of $M(H)$ show the onset of the metamagnetic transition at all pressures. Since the applied magnetic field is not enough to achieve saturation, the typical S-shape magnetization characteristic is not observed. A similar behavior was also found for the nanocrystalline MnP in the phosphide chalcopyrite, as well as for bulk MnP forms [33], evidencing that the saturation at $T = 300$ K occurs at higher fields.

We defined the critical field H_C for the onset of the metamagnetic transition as an inflection point in dM/dH , as shown in Fig. 3 (lower panels). The variation of H_C at compression within the offset of P^{\max} is illustrated on the

contour map [see the inset to Fig. 2(a)]. A corresponding line on the contour map presents the boundary between the two magnetic states with low and high magnetization. This implies that the maxima of P^{\max} from Fig. 2(a) are associated with antiferromagnetic and ferromagnetic orderings below and above H_C , respectively.

The pressure dependencies of H_C at compression and decompression are plotted in Fig. 4. It should be noted that even the roughly estimated slope for pressure coefficient dH_C/dP in both pressure directions shows different changes in its rate and sign in the vicinity of P^{\max} at 5 kOe. For example, the rate and the sign of the slope are -0.23 kOe/GPa and $+0.09$ kOe/GPa at compression and -0.38 kOe/GPa and $+0.2$ kOe/GPa at decompression, respectively. From this

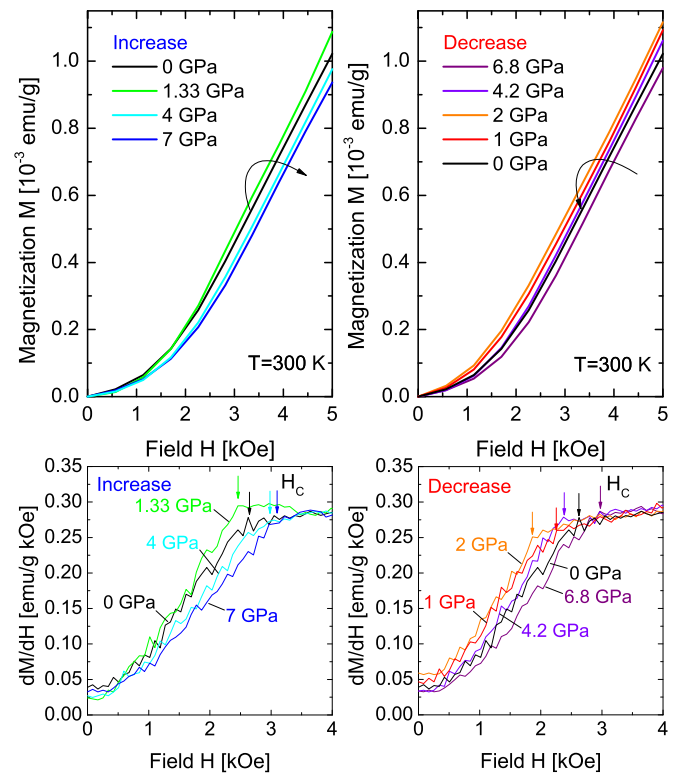


FIG. 3. Magnetization isotherms (upper panels) and their derivatives dM/dH (lower panels) at different applied pressures measured at compression (left) and decompression (right). Curly arrows indicate the dynamics of $M(H)$ curves from ambient pressure up to 7 GPa and vice versa. The critical fields of H_C corresponding to the onset of the metamagnetic transition are denoted by vertical arrows.

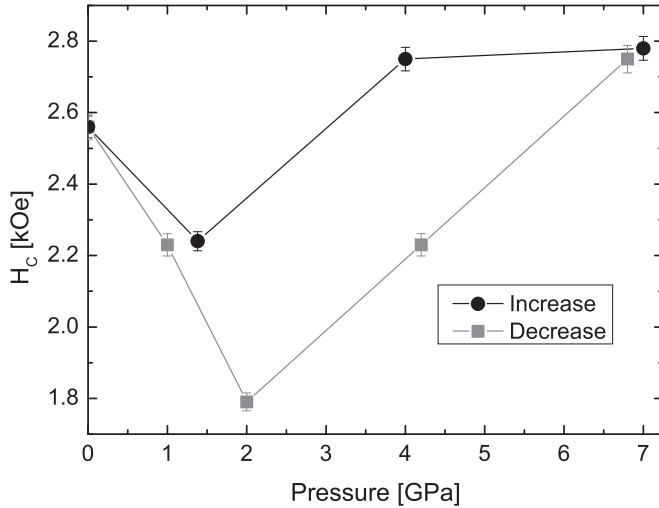


FIG. 4. Pressure dependence of H_C at compression and decompression.

analysis, it can be argued that the positive slope of H_C indicates the antiferromagnetic spin configuration of the MnP cluster, while a negative slope is due to the increasing population of ferromagnetically aligned clusters. Moreover, the hysteretic behavior of H_C versus pressure is consistent with the results shown in Fig. 3, clearly indicating a reversible metamagnetic transition.

Generalizing all these data, one may conclude that the maximum magnetization at $P^{\max} = 3.5$ GPa can be interpreted as the formation of a pressure-induced antiferromagnetic configuration for MnP clusters starting from zero fields. This observation of antiferromagnetic ordering under pressure is not surprising. Actually, as debated over the years, a bulk MnP crystal exhibits a feature associated with the transition from the ferromagnetic to antiferromagnetic phase above $P \sim 3$ GPa [34,35]. In the orthorhombic MnP structure, Mn spins aligned along the crystallographic c axis form a ferromagnetic phase at $T_C < 291$ K [36]. In the helical or screw phase below $T_h = 50$ K [36], the spin spiral rotates in the bc plane with propagation vector \mathbf{q} along the a axis. The helical structure is recognized to be responsible for the metamagnetic state, which includes both ferromagnetic and antiferromagnetic interactions. As reported by Hirahara *et al.* [37], the effects of uniaxial compression along the a axis enhance the antiferromagnetic interaction relative to the ferromagnetic one, with a weak increase in T_h and decrease in T_C . The strong decrease in dT_C/dP by about -18.5 K/GPa has also been confirmed by several hydrostatic pressure studies [35,38,39]. Thus, concerning our situation, the probability for ferromagnetic ordering of MnP clusters at $P^{\max} = 3.5$ GPa will be perhaps eliminated. Meanwhile, the antiferromagnetic state of the MnP clusters seems very mysterious, since it would result in a giant shift in T_h toward room temperatures. However, if we accept a scenario of pressure-induced ferromagnetic-to-antiferromagnetic transition, its nature can be explained by Goodenough's narrow $3d$ -band model [40]. Likewise for MnAs (B31), the MnP orthorhombic lattice can be treated as a low-spin state [41] in which the ferromagnetic interaction is due to itinerant electrons, while the antiferromagnetic

spin-density wave is caused by indirect exchange between the localized electrons of Mn ions and nonmagnetic P ions. Since the density of states near the Fermi level is basically attributed to the itinerant electrons, the interaction between the Mn-Mn bonds lengths will more sensitive to pressure than the Mn-P-Mn interaction. Therefore, a pressure-induced ferromagnetic-to-antiferromagnetic transition may arise due to bandwidth broadening in the narrow $3d$ -band of MnP [34,40].

The outcome discussed here seems appropriate for our case if the initial state for MnP clusters is ferromagnetic [42]. Given that the system of submicron MnP clusters consists of a large number of crystallites, and their crystal axes are misoriented with respect to each other in the CdGeP₂ matrix, a zero-field ground state should not be ferromagnetic, but is very likely to be superparamagnetic-like. Following the observation of the low-field-induced metamagnetic behavior (Fig. 3), the opposite antiferromagnetic-to-ferromagnetic transition occurs even at ambient pressure. This characteristic does not weaken qualitatively with increasing pressure. Hence, the pressure-induced antiferromagnetic state for MnP clusters has a different origin that likely does not meet the criteria of bandwidth broadening [40]. As our results suggested, the applications of low magnetic field and high pressure equally induce the antiferromagnetic type for MnP clusters. Its mechanism may be understood in terms of field-induced spin reconfiguration of superparamagnetic-like clusters, while the hydrostatic pressure effect at zero fields is due to changes in the interatomic distances. According to calculations based on density functional theory for the $Pnma$ structure of MnP [43], the distance $d_1 \geq 2.95$ Å was defined for ferromagnetic coupling ($d_1 \leq 2.95$ Å for antiferromagnetic coupling) between the shortest Mn-Mn separation along the c axis, which plays a key role in determining the exchange interaction. It should be noted that only lattice parameters for bulk MnP were considered, while the similar value of d_1 for MnP clusters may vary. We experimentally estimated that the lattice constants for the orthorhombic structure of MnP clusters show a slight decrease in comparison with the bulk MnP [35,36]. This leads to the assumption that for given lattice parameters, it is favorable to reconfigure MnP clusters into the antiferromagnetic type via external perturbation (pressure or magnetic field).

Our experimental findings on the magnetic changes of MnP clusters in an insulating CdGeP₂ matrix are summarized in the P - H phase diagram (Fig. 5). In the pressure range up to 7 GPa, the mixed color area of the reversible metamagnetic transition, highlighted as hysteresis of H_C , provides a distinct boundary between the antiferromagnetic and the ferromagnetic states. The diagram shows that a strong antiferromagnetic state is induced by pressure at $P \approx 3.5$ GPa and, with the field increase, tends toward the ferromagnetic region through the metamagnetic transition. In addition, the colored area of the antiferromagnetic state involves the superparamagnetic-like contribution, the borders of which are defined conditionally. However, the presented superparamagnetic-like state is not clarified in detail yet, but it is typical for hybrid systems with a chalcopyrite matrix [30]. We propose that such a state can exist within a narrow range of pressures and magnetic fields, and so a slight increase in P or H will reconfigure the clusters into the antiferromagnetic state.

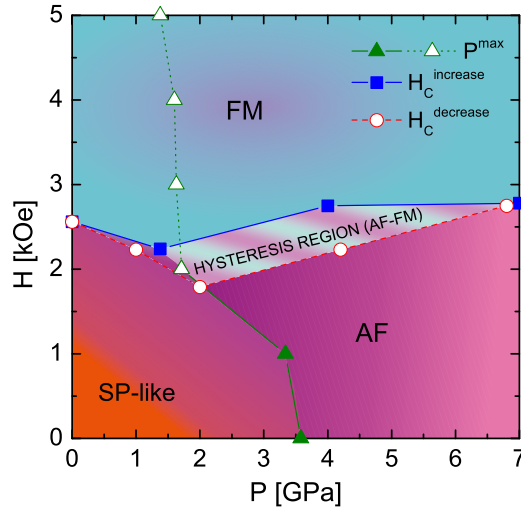


FIG. 5. Magnetic field–pressure phase diagram of MnP clusters in the CdGeP₂ matrix, including hysteresis region of H_C and the magnetization data P^{\max} . AF denotes the antiferromagnetic, FM denotes the ferromagnetic, and SP denotes the superparamagnetic-like state. The closed and open triangles are variation in P^{\max} from the antiferromagnetic to the ferromagnetic state, respectively.

The pressure evolution and low-field evolution of the MnP clusters (superparamagnetic-like–antiferromagnetic–metamagnetic–ferromagnetic) are components for understanding the unusual hysteresis [Fig. 2(b)]. As has been mentioned, the reason for inversion of the magnetization hysteresis direction in Mn-doped ZnGeAs₂ was associated with the competing interaction between two types of MnAs clusters at the structural transition in the semiconducting ZnGeAs₂ [27]. Because CdGeP₂-MnP has one orthorhombic type of MnP cluster, and the surrounding matrix of CdGeP₂ is insulating, a competing mechanism does not necessarily exist. This supports the interpretation that the major contribution to the unusual hysteresis is related to the structural transition of the host. As is evident from Fig. 6, a volume jump in V/V_0 of $\sim 1.8\%$ is observed at $P = 5.28$ GPa, which is the signal for the structural transition. In addition, the structural transition is also supported by observation of hysteresis at the decompression point. We adopt the third-order Birch-Murnaghan equation of state [44] for derivation of the values of the bulk modulus B_0 for each observed phase,

$$P(V) = \frac{3B_0}{2} \left[\left(\frac{V}{V_0} \right)^{-\frac{7}{3}} - \left(\frac{V}{V_0} \right)^{-\frac{5}{3}} \right] \times \left[1 + \frac{3}{4}(B'_0) \left(\left(\frac{V}{V_0} \right)^{-\frac{2}{3}} - 1 \right) \right], \quad (1)$$

where P , V , and V_0 are pressure, volume at pressure P , and volume at ambient pressure, respectively. B_0 and B'_0 are the bulk modulus at zero pressure and its pressure derivative. The result of the fitting procedure yields the values $B_0 = 87 \pm 2$ GPa, $B'_0 = 4$, and $B_0 = 91 \pm 1$ GPa, $B'_0 = 4$ for the initial and high-pressure polymorph phase, respectively.

Without specifying this structural transition, one can be sure that the values of B_0 are always overestimated, whether or not the value of B_0 for the initial phase of CdGeP₂ is different from

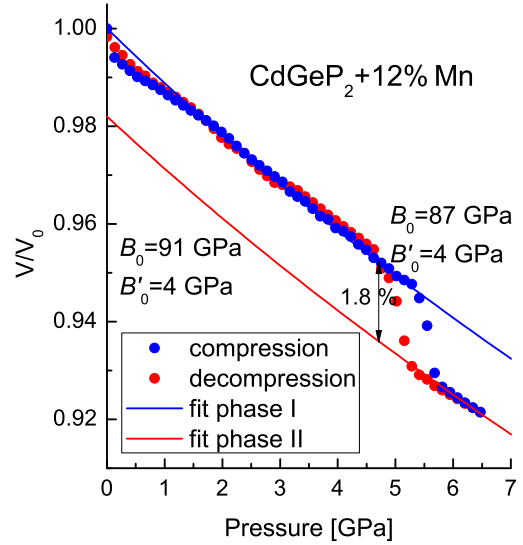


FIG. 6. The volume changes for CdGeP₂-MnP under pressure. The hysteresis is observed at decompression, evidencing a structural transition. The solid lines represent the results of fitting based on third-order Birch-Murnaghan equation of state.

the pure chalcopyrite structure [45]. Despite this difference, the effect caused by polymorphism of the matrix still has a significant influence on the magnetic behavior of the MnP clusters. In particular, the divergence of the magnetization hysteresis at decompression [Fig. 2(b)] occurs at the same pressure value, which coincides with the beginning of the structural transition ($P = 5.28$ GPa). It is clear that the volume behavior of the sample is sensitive to the presence of clusters, the contributions of which cannot be ignored. Allocation of the clusters' contribution from the overall structural changes is a puzzling question that is also complicated for composite systems using high-pressure XRD methods [46].

Accordingly, the pressure-induced unusual magnetization hysteresis may be generally understood through the difference in bulk compressibility of the CdGeP₂ matrix and MnP clusters. The impact of pressure on the properties of clusters through the matrix leads to nonuniform structure recovery of both clusters and matrix components at decompression. In particular, the relaxation of the clusters becomes pronounced owing to the structural transition. This behavior is also reflected in the difference in pressure coefficients dH_C/dP at compression and decompression. Besides the clusters' compressibility, a number of factors, including their electronic and magnetic structure, defect states, effect of grain boundaries, etc., will influence the degree of the clusters' response. Here, we point out that the stimulating force for the unusual hysteresis is related to the pressure-induced antiferromagnetic state of the MnP clusters in zero magnetic field, while its enhancement occurs due to the metamagnetic transition in fields of $H = 2\text{--}5$ kOe according to the variation in H_C (Fig. 4).

In summary, we investigated the effect of hydrostatic pressure and low magnetic field on the MnP clusters in an insulating CdGeP₂ matrix at room temperature. At compression, we observed features at $P \approx 3.5$ GPa associated with pressure-

induced antiferromagnetic ordering of the MnP clusters at zero field, which was previously attributed to the bulk form of MnP [34]. A similar effect was achieved by applying low field, further supported by the onset of the field-induced metamagnetic transition. The effect of pressure cycling on the magnetization uncovered an unusual hysteresis phenomenon produced by the MnP clusters. An enhancement of this hysteresis at low fields indicates an underlying reversible metamagnetic behavior. Such unusual characteristics most probably are caused by the pressure-induced structural transition at $P = 5.28$ GPa, which gives rise to a distinct difference in the bulk properties of

the host matrix and clusters. Although our paper does not cover all physical aspects, particularly, in the field of the structural transition, we believe that our results will facilitate understanding of unexpected cluster properties, including their self-organization in hybrid systems.

The authors would like thank Z. Gercsi for useful discussions and remarks on this manuscript. This paper was supported by the Russian Foundation for Basic Research (Grants No. 16-02-00210 a, No. 16-32-00661 mol_a, and No. 16-03-00796 a) and the RAS Presidium Program I.11 Π.

-
- [1] T. Dietl, *Nat. Mater.* **9**, 965 (2010).
- [2] S. Kuroda, N. Nishizawa, K. Takita, M. Mitome, Y. Bando, K. Osuch, and T. Dietl, *Nat. Mater.* **6**, 440 (2007).
- [3] H. Akinaga, *Semicond. Sci. Technol.* **17**, 322 (2002).
- [4] T. Y. Chen, S. X. Huang, C. L. Chien, and M. D. Stiles, *Phys. Rev. Lett.* **96**, 207203 (2006).
- [5] M. Jamet, A. Barski, T. Devillers, V. Poydenot, R. Dujardin, P. Bayle-Guillemaud, J. Rothman, E. Bellet-Amalric, A. Marty, J. Cibert, R. Mattana, and S. Tatarenko, *Nat. Mater.* **5**, 653 (2006).
- [6] K. W. Liu, J. Y. Zhang, D. Z. Shen, X. J. Wu, B. H. Li, B. S. Li, Y. M. Lu, and X. W. Fan, *Appl. Phys. Lett.* **90**, 092507 (2007).
- [7] I.-S. Yu, M. Jamet, T. Devillers, A. Barski, P. Bayle-Guillemaud, C. Beigné, J. Rothman, V. Baltz, and J. Cibert, *Phys. Rev. B* **82**, 035308 (2010).
- [8] G. Monette, C. Lacroix, S. Lambert-Milot, V. Boucher, D. Ménard, and S. Francoeur, *J. Appl. Phys.* **107**, 09A949 (2010).
- [9] H. Akinaga, S. Miyayoshi, K. Tanaka, W. Van Roy, and K. Onodera, *Appl. Phys. Lett.* **76**, 97 (2000).
- [10] D. D. Dung and S. Cho, *J. Appl. Phys.* **113**, 17C734 (2013).
- [11] S. Serrano-Guisan, G. di Domenicantonio, M. Abid, J.-P. Abid, M. Hillenkamp, L. Gravier, J.-P. Ansermet, and C. Félix, *Nat. Mater.* **5**, 730 (2006).
- [12] P. N. Hai, Y. Sakata, M. Yokoyama, S. Ohya, and M. Tanaka, *Phys. Rev. B* **77**, 214435 (2008).
- [13] P. N. Hai, S. Ohya, M. Tanaka, S. E. Barnes, and S. Maekawa, *Nature (London)* **458**, 489 (2009).
- [14] B. Rache Salles, J. C. Girard, C. David, F. Offi, F. Borgatti, M. Eddrief, V. H. Etgens, L. Simonelli, M. Marangolo, and G. Panaccione, *Appl. Phys. Lett.* **100**, 203121 (2012).
- [15] M. Moreno, V. M. Kaganer, B. Jenichen, A. Trampert, L. Däweritz, and K. H. Ploog, *Phys. Rev. B* **72**, 115206 (2005).
- [16] M. Tanaka, *Semicond. Sci. Technol.* **17**, 327 (2002).
- [17] H.-A. Krug von Nidda, T. Kurz, A. Loidl, Th. Hartmann, P. J. Klar, W. Heimbrod, M. Lampalzer, K. Volz, and W. Stolz, *J. Phys.: Condens. Matter* **18**, 6071 (2006).
- [18] D. W. Rench, P. Schiffer, and N. Samarth, *Phys. Rev. B* **84**, 094434 (2011).
- [19] M. T. Elm, P. J. Klar, S. Ito, and S. Hara, *Phys. Rev. B* **83**, 235305 (2011).
- [20] M. T. Elm, P. J. Klar, S. Ito, S. Hara, and H.-A. Krug von Nidda, *Phys. Rev. B* **84**, 035309 (2011).
- [21] C. Michel, M. T. Elm, B. Goldlücke, S. D. Baranovskii, P. Thomas, W. Heimbrod, and P. J. Klar, *Appl. Phys. Lett.* **92**, 223119 (2008).
- [22] T. R. Arslanov, A. Yu. Mollaev, I. K. Kamilov, R. K. Arslanov, L. Kilanski, V. M. Trukhan, T. Chatterji, S. F. Marenkin, and I. V. Fedorchenko, *Appl. Phys. Lett.* **103**, 192403 (2013).
- [23] T. R. Arslanov, A. Yu. Mollaev, I. K. Kamilov, R. K. Arslanov, L. Kilanski, R. Minikaev, A. Reszka, S. López-Moreno, A. H. Romero, M. Ramzan, P. Panigrahi, R. Ahuja, V. M. Trukhan, T. Chatterji, S. F. Marenkin, and T. V. Shoukavaya, *Sci. Rep.* **5**, 7720 (2015).
- [24] H. Zhang, F. Ke, Y. Li, L. Wang, C. Liu, Y. Zeng, M. Yao, Y. Han, Y. Ma, and Ch. Gao, *Sci. Rep.* **5**, 14417 (2015).
- [25] V. Moshnyaga, B. Damaschke, O. Shapoval, A. Belenchuk, J. Faupel, O. I. Lebedev, J. Verbeeck, G. Van Tendeloo, M. Mücksch, V. Tsurkan, R. Tidecks, and K. Samwer, *Nat. Mater.* **2**, 247 (2003).
- [26] M. Baldini, T. Muramatsu, M. Sherafati, H. Mao, L. Malavasi, P. Postorino, S. Satpathy, and V. V. Struzhkin, *PNAS*, **112**, 10869 (2015).
- [27] T. R. Arslanov, L. Kilanski, S. López-Moreno, A. Yu. Mollaev, R. K. Arslanov, I. V. Fedorchenko, T. Chatterji, S. F. Marenkin, and R. M. Emirov, *J. Phys. D: Appl. Phys.* **49**, 125007 (2016).
- [28] J. Dho, W. S. Kim, and N. H. Hur, *Phys. Rev. Lett.* **87**, 187201 (2001).
- [29] V. M. Novotortsev, S. A. Varnavskii, S. F. Marenkin, L. I. Koroleva, R. V. Demin, V. M. Trukhan, S. O. Klimonskii, and V. D. Kuznetsov, *Russian J. Inorg. Chem.* **51**, 1153 (2006).
- [30] I. V. Fedorchenko, L. Kilanski, I. Zakharchuk, P. Geydt, E. Lahderanta, P. N. Vasilyev, N. P. Simonenko, A. N. Aronov, W. Dobrowski, and S. F. Marenkin, *J. Alloy. Compd.* **650**, 277 (2015).
- [31] L. G. Khvostantsev, V. N. Slesarev, and V. V. Brazhkin, *High Pressure Res.* **24**, 371 (2004).
- [32] O. B. Tsiok, L. G. Khvostantsev, A. V. Golubkov, I. A. Smirnov, and V. V. Brazhkin, *Phys. Rev. B* **90**, 165141 (2014).
- [33] J. A. Aitken, G. M. Tsoi, L. E. Wenger, and S. L. Brock, *Chem. Mater.* **19**, 5272 (2007).
- [34] M. D. Banus, *J. Solid State Chem.* **4**, 391 (1972).
- [35] J.-G. Cheng, K. Matsubayashi, W. Wu, J. P. Sun, F. K. Lin, J. L. Luo, and Y. Uwatoko, *Phys. Rev. Lett.* **114**, 117001 (2015).
- [36] E. E. J. Huber and H. D. Ridgley, *Phys. Rev.* **135**, A1033 (1964).
- [37] E. Hirahara, T. Suzuki, and Y. Matsumura, *J. Appl. Phys.* **39**, 713 (1968).
- [38] N. P. Grazhdankina, A. M. Burkhanov, and Y. S. Bersenev, *Zh. Eksp. Teor. Fiz.* **55**, 2155 (1968) [*Sov. Phys. JETP* **28**, 1141 (1969)].

- [39] T. Kamigaich, T. Okamoto, N. Iwata, and E. Tatsumoto, *J. Phys. Soc. Jpn.* **24**, 649 (1968).
- [40] J. B. Goodenough, in *Progress in Solid State Chemistry*, edited by H. Reiss (Pergamon Press, Oxford, 1971), Chap. 4.
- [41] N. Menyuk, J. A. Kafalas, K. Dwight, and J. B. Goodenough, *J. Appl. Phys.* **40**, 1324 (1969).
- [42] Although preliminary data for the temperature-dependent magnetization point out a slight difference in the Curie temperature of $T_C \sim 335$ K, comparable with the composition of 5% Mn ($T_C \sim 332$ K [23]), the measured magnetic field was superior to that used in the present paper.
- [43] Z. Gercsi and K. G. Sandeman, *Phys. Rev. B* **81**, 224426 (2010).
- [44] F. Birch, *Phys. Rev.* **71**, 809 (1947).
- [45] A. S. Verma, *Mat. Chem. Phys.* **139**, 256 (2013).
- [46] K. E. Lipinska-Kalita, P. E. Kalita, C. Gobin, O. A. Hemmers, T. Hartmann, and G. Mariotto, *Phys. Rev. B* **77**, 134107 (2008).